Supplemental Data

Supplemental Figures Legends

Suppl. Figure 1. **PPAR expression in the embryonic and adult pancreas and co-localization with insulin.**

(A) Relative *Ppara* mRNA expression levels in the pancreas at different stages of fetal and postnatal life ($n = 4$); ***$p < 0.007$. **(B)** *Pparg* mRNA levels in the same conditions than **(A)** ($n = 4$); *$p < 0.05$, **$p < 0.01$. **(C)** Relative *Pparb/d* mRNA expression levels in total pancreas and isolated islets ($n = 5$); *$p < 0.05$. **(D)** TaqMan analysis of RNA expression of *Pparb/d* in pancreas from *Pparb/d*$^{fl/fl}$ (control, C) and Pdx1Cre;*Pparb/d*$^{fl/fl}$ (KO) 8-week-old mice ($n = 3$); ***$p = 10^{-15}$. **(E)** Expression of PPARβ/δ (red) and insulin (green) by immunostaining in pancreas from E17.5 embryos. DAPI in blue. Scale bar: 50 μm. **(F)** TaqMan analysis of RNA expression of *Ppara* in islets and pancreas from *Pparb/d*$^{fl/fl}$ (control, C) and Pdx1Cre;*Pparb/d*$^{fl/fl}$ (KO) 8-week-old mice ($n = 3$); NS = not significant. **(G)** *Pparg* mRNA levels in the same conditions than **(F)** ($n = 3$).

Suppl. Figure 2. Insulin- and Neurog3-expressing cell populations and Neurog3 protein amount in embryonic pancreata; glucagon levels and α- and β-cell mass in adult pancreata.

(A) Quantification of insulin expressing cells in embryonic day 15.5 pancreas; insulin-stained cells were normalized with e-cadherin expressing cells (area) ($n = 3$). **(B)** RNA expression level of *Insulin I* in E15.5 pancreas, measured by qRT-PCR ($n = 8$). **(C)** Quantification of Neurog3 expressing cells in the same conditions as (A) ($n = 3$). **(D)** RNA expression level of *Neurog3* in the same conditions as (B) ($n = 3$). **(E)** Left panel: Neurog3 protein level in

pancreas from *Pparb/d*$^{fl/fl}$ (control, C) and Pdx1Cre;*Pparb/d*$^{fl/fl}$ (KO) mice at two embryonic stages (E17.5 and E18.5). Right panel: quantification of the blot of left panel. **(F)** Quantification of α-cell mass from 8-week-old *Pparb/d*$^{fl/fl}$ (control, C) and Pdx1Cre;*Pparb/d*$^{fl/fl}$ (KO) mice (n = 3); *p < 0.05. **(G)** Glucagon content in pancreas from *Pparb/d*$^{fl/fl}$ (control, C) and Pdx1Cre;*Pparb/d*$^{fl/fl}$ (KO) 8-week-old mice (n = 6); NS = not significant. **(H)** Glucagon content in islets from *Pparb/d*$^{fl/fl}$ (control, C) and Pdx1Cre;*Pparb/d*$^{fl/fl}$ (KO) 8-week-old mice (n = 4); NS = not significant. **(I)** Representative *Pparb/d*$^{fl/fl}$ (control, C) and Pdx1Cre;*Pparb/d*$^{fl/fl}$ (KO) pancreas sections stained with anti-insulin antibody. Scale bar: 1 mm.

Suppl. Figure 3. Intracellular Ca^{2+} measurement and GSIS from PPARβ/δ deficient islets.

(A) Free intracellular Ca^{2+} measurement from dissociated *Pparb/d*$^{fl/fl}$ (control, C) and Pdx1Cre;*Pparb/d*$^{fl/fl}$ (KO) islets in glucose- (3 vs. 17 mM) and KCl- (3.6 vs. 50 mM) stimulated conditions. Graph of AUC **(B)** and height **(C)** of response to stimulation (n = 18 cells from 3 mice). AU, arbitrary units. **(D)** Left graph: Relative *Pparb/d* mRNA expression in Ad-shRNA-Control and Ad-shRNA-PPARβ/δ adenovirus infected CBL57/6J islets used in GSIS mentioned on the right graph (n = 4); **p < 0.05. Right graph: GSIS in adenovirus-infected islets isolated from CBL57/6J mice. The islets were infected either with adenovirus control containing scrambled shRNA (control) or adenovirus containing shRNA against *Pparb/d* the GSIS was performed 72 after the infection as mentioned in the experimental procedures (n = 4); ***p < 0.005. **(E)** Left graph: Relative *Pparb/d* mRNA expression in adenovirus infected islets used in GSIS shown in the right graph (n = 3); **p < 0.05. Right graph: 16.7 mM glucose-stimulated insulin secretion in adenovirus-infected islets from Pdx1Cre;*Pparb/d*$^{fl/fl}$ (KO) mice. The islets were infected either with adenovirus containing

human PPARβ/δ coding sequences under CMV promoter (ad-CMV-PPARβ/δ) or adenovirus containing CMV-GFP construction (ad-control), GSIS was performed as in (D) (n = 3); **$p < 0.05$.

Suppl. Figure 4. F- and G-actin in *Pparb/d*$^{fl/fl}$ (Control) and Pdx1Cre;*Pparb/d*$^{fl/fl}$ (KO) isolated islets.

Matrix-plated islets were stained against F-actin with phalloidin rhodamine (Invitrogen) and G-actin by using DNase I Fluor 488 (Invitrogen). The nuclei were stained with DNase I, indicating the presence of G-actin, as reported previously (1). Scale bar: 50 μm.

Suppl. Figure 5. Effect of PKD1 inhibitor on the organization of Golgi apparatus in PPARβ/δ deficient islets.

(A) Immunostaining of the *trans* Golgi marker TGN 38 (green) in islets from *Pparb/d*$^{fl/fl}$ (control, C) and Pdx1Cre;*Pparb/d*$^{fl/fl}$ (KO) mice. **(B)** Effect of PKD1 inhibitor, Gö6976 (Go), on Golgi apparatus in islets from control and KO mice. The immunostaining of giantin (red) labels the Golgi apparatus. DAPI (blue). Scale bar: 20μm. **(C)** Quantification of giantin stained areas in islets treated with Go during 12h (Go) and untreated (NT) (n = 10-15 islets from 3 mice); **$p < 0.005$, ***$p < 10^{-10}$. **(D)** Giantin protein level in control and KO islets.

Supplemental Figure 1.

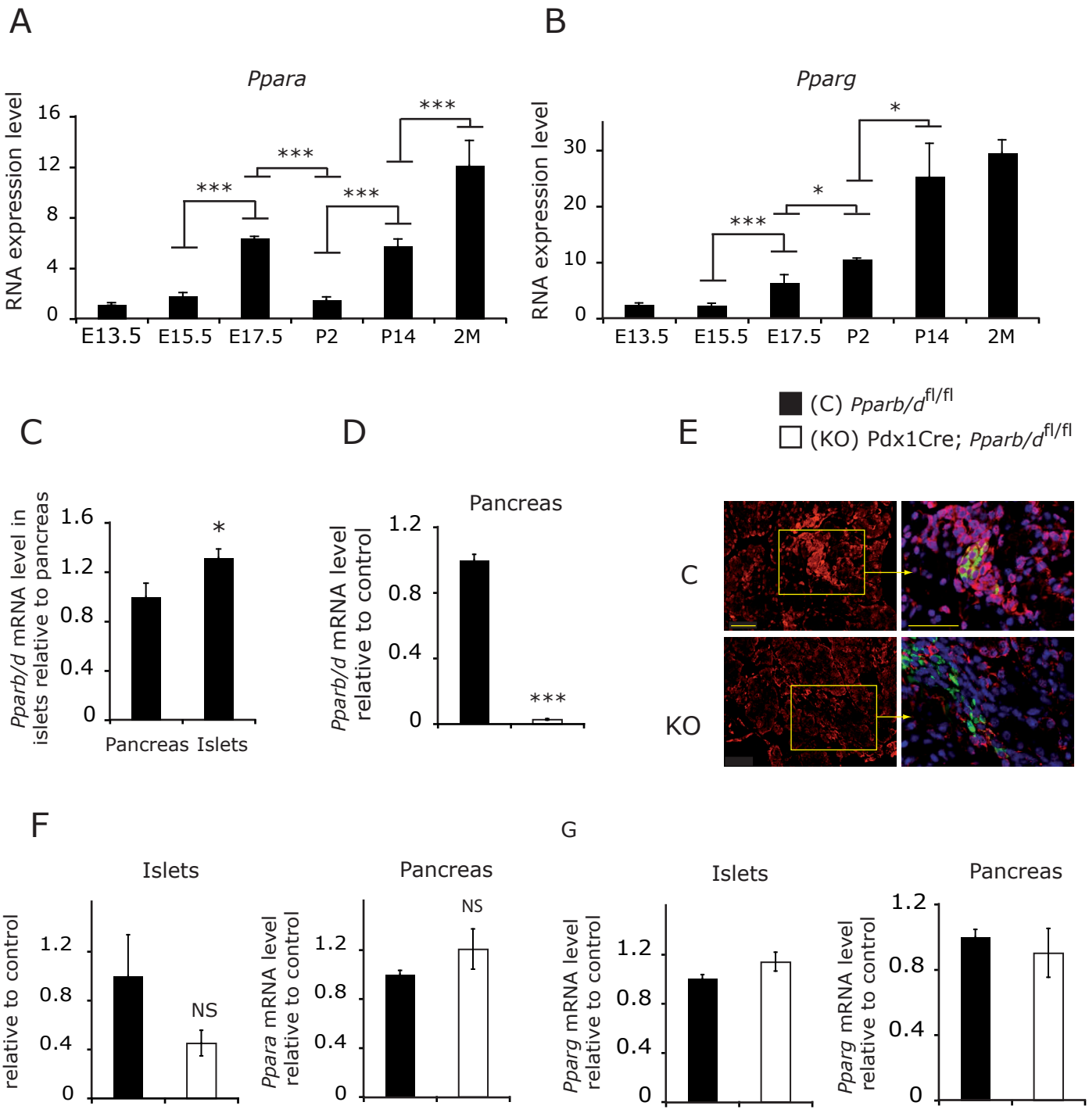

Supplemental Figure 2.

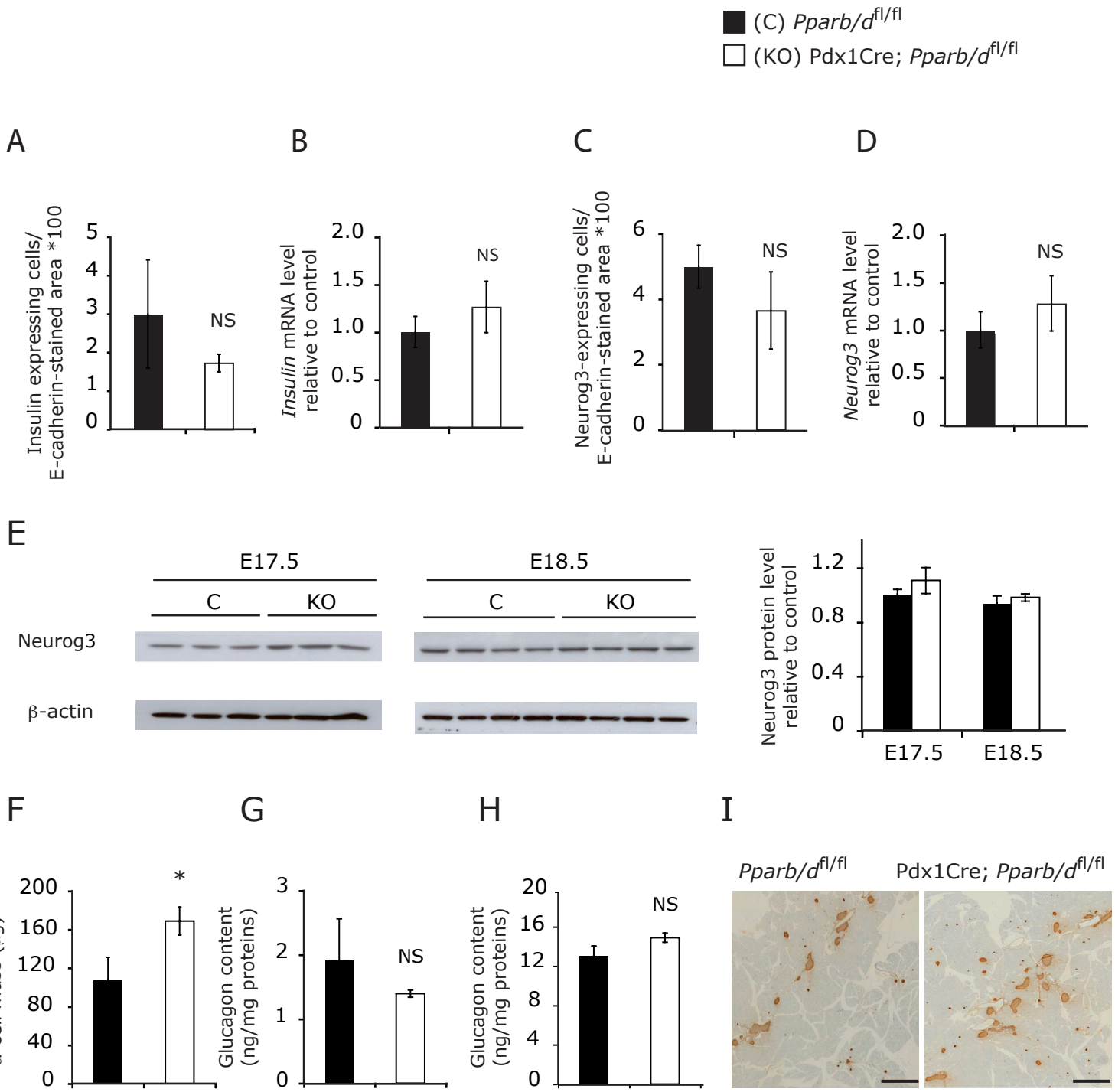

Supplemental Figure 3.

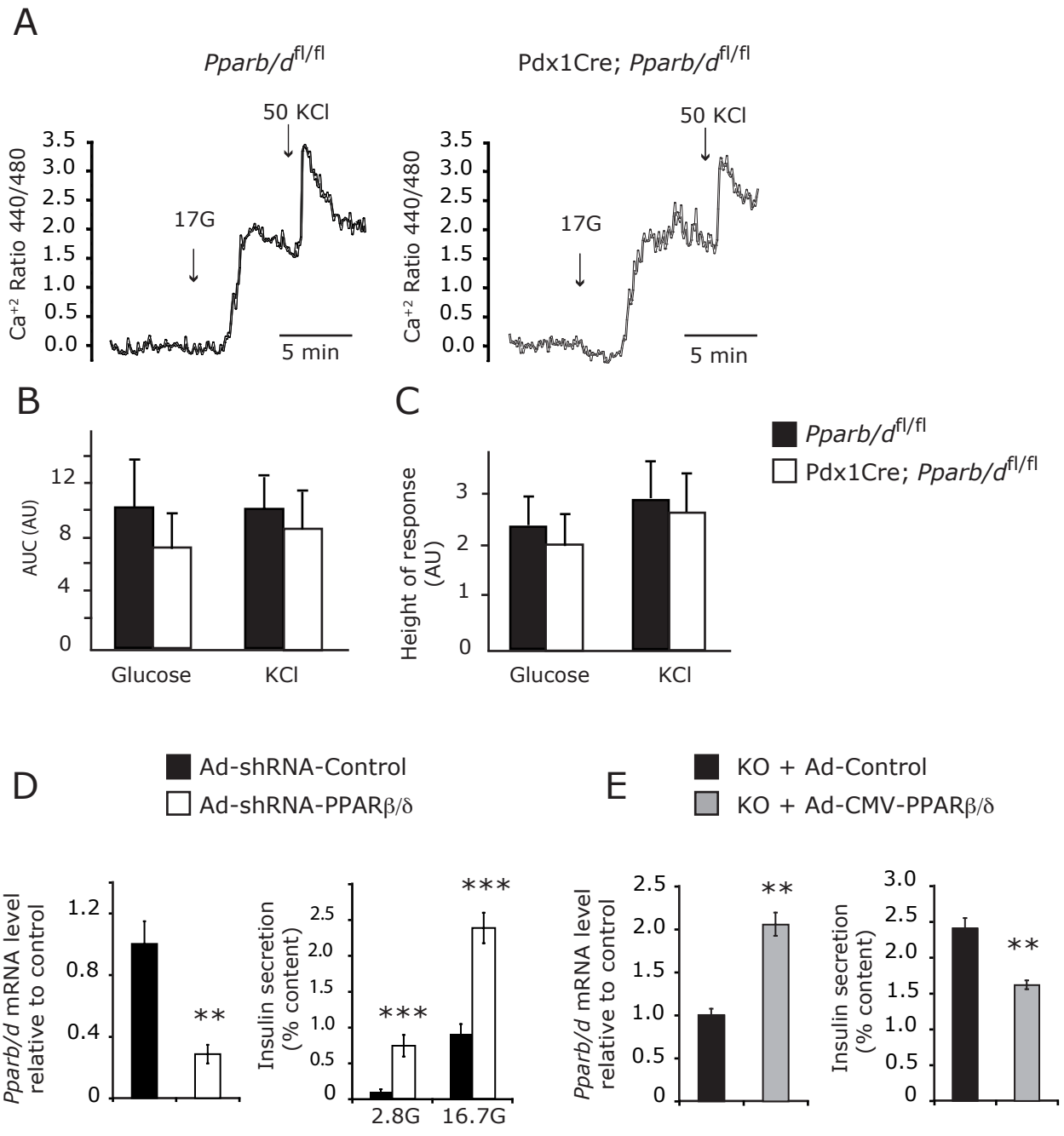

Supplemental Figure 4.

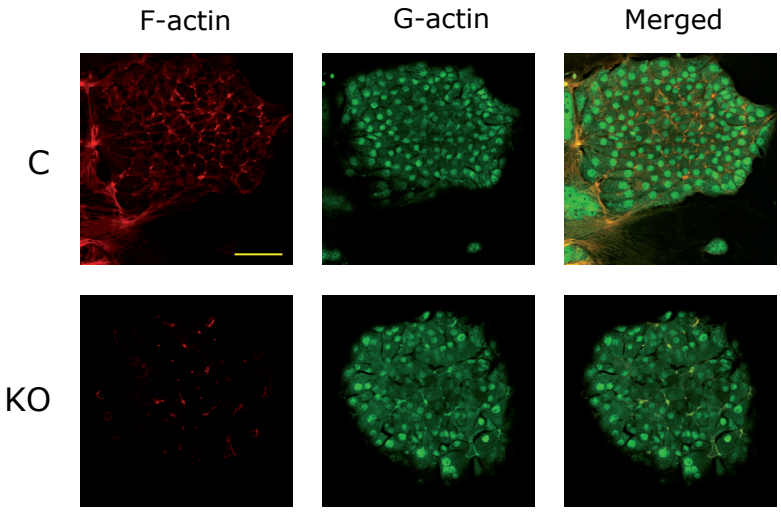

Supplemental Figure 5.

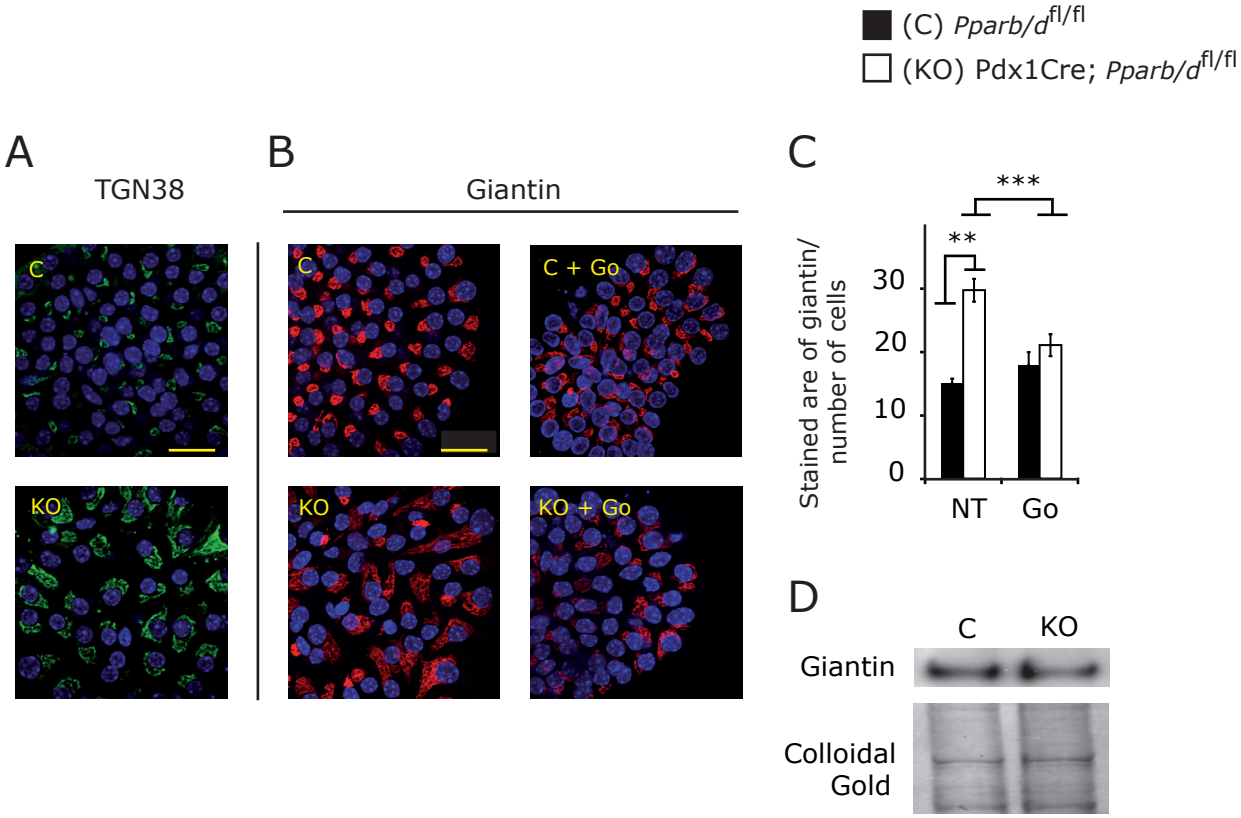

Supplemental Table 1. Fold change (FC) of PPARs, differentiated and precursors endocrine markers expression between PPARβ/δ deficient and control pancreas at postnatal stages

	P3		P14	
Symbol	FC	t-test	FC	t-test
PPARα	-1.23049756	NS	-1.13340572	0.02514891
PPAR β/δ	-6.08490975	4.7898E-09	-9.40179906	8.5639E-11
PPARγ	-0.52235041	NS	-0.37653764	NS
Glucagon	-2.82786619	NS	3.38990002	0.02109872
InsI	2.47556877	0.00811159	8.89706459	5.7513E-07
InsII	-0.11440893	NS	2.81375094	0.00041674
Sst	1.54547959	NS	1.31322911	NS
Pdx1	0.65489487	NS	4.80031991	2.9056E-07
Neurog3	-3.3234005	0.00330301	-7.43768898	3.2577E-07
NeuroD	-3.08986113	NS	6.37959569	0.00018235
Nkx2-2	0.51585672	NS	5.61593277	0.00430985
Pax6	-2.77234528	NS	2.96381988	0.00061784
Brn4	-4.00223617	NS	-3.18858871	0.00140956
Isl1	-1.23095063	NS	3.63326736	0.0004099
P48	1.14276677	NS	0.43357942	NS

Gene expression was determined from total pancreas RNA at postnatal day 3 (P3) and 14 (P14) by TaqMan. t-test we compared two groups and assumed a two-tailed distribution and unequal variance. n=5. NS = Non significant

Supplemental Table 2. GO enrichment term

Cut-off	Direction	Term	Obs	Exp	Pval	Genes
FDR 10%	UP	adhesion	17	11.5207101	0.07257204	Tgm2, Cldn1, Cpxm2, Ttyh1, Cldn2, Cml2, Cdh17, Itga6, Cldn8, B4galt1, Pcdha1, Amigo2, F8, Icam1, Tgfbi, Igfals, Cntn3
FDR 10%	UP	apoptosis	17	13.883432	0.2292618	Cradd, Nek6, Elmo1, Igfbp3, Ngfr, Hif1a, Asah2, Cln8, Tnfrsf11b, B4galt1, Il6, Acvr1c, Chpt1, Sgms1, Casp3, Tnfaip8, Bcl2a1a
FDR 10%	UP	cell cycle	13	12.7899408	0.51581077	Tpd52l1, Nek6, Cdc14a, Zwint, Ttyh1, Id4, Cks1b, Loh11cr2a, Araf, Jun, Smarcb1, Casp3, Syce2
FDR 10%	UP	cell differentia	16	14.8792899	0.41915301	Hopx, Hrb, Xdh, Rasgrp1, Morc1, Ngfr, Tnfaip2, Hif1a, Pappa, Efnb2, Il6, Acvr1c, Jun, Smarcb1, Sema4d, Efna5
FDR 10%	UP	cell junction	11	6.48284024	0.0625105	Cldn1, Panx1, Rph3a, Cldn2, Cldn8, Itsn1, Dlg2, Scamp5, Synpr, Gad2, Syt10
FDR 10%	UP	cytoskeleton	14	9.64615385	0.10648961	Palld, Pstpip2, Sntg2, Elmo1, Epb4.1l4a, Mylk, Rph3a, Myo3a, Wipf1, Enc1, Cttnbp2, Svil, Dnm3, Tbcel
FDR 10%	UP	development	40	33.1366864	0.12401304	Hopx, Wnt5b, G6pd2, Prrx1, Prr15, Runx1, Dkk3, Scn9a, Fzd3, Grhl1, Hrb, Morc1, Ngfr, Id4, Cml2, Fzd4, Ppp2r2b, Tnfaip2, Hif1a, Gfra3, Dct, Efnb2, Ugcg, Myo5a, Cln8, Slc39a6, Bptf, B4galt1, Slc5a3, Acvr1c, Smarcb1, Fgfr2, Casp3, Sftpd, Thbd, Enc1, Crybb3,
FDR 10%	UP	endoplasmic re	28	15.3674556	0.00177466	Fmo1, Edem3, Ugt1a1, Acsl4, H13, Minpp1, P4ha1, Rasgrp1, Tap2, Sqle, Cml2, Cldn8, Ugcg, Stch, Cln8, Slc39a6, Tmed5, Serinc5, Atf6, Sgms1, Soat1, Mcfd2, Txndc4, Apob, Trappc2, B3galt5, Edem1, Ero1l
FDR 10%	UP	fatty acid	7	2.94852071	0.02906126	Acadsb, Acot12, Acsl4, Acsf2, Myo5a, Fabp4, Ehhadh
FDR 10%	UP	Golgi	52	25.8532544	1.27E-06	Chst9, Chst9, Wipi1, Wipi1, St3gal3, St3gal3, Rasgrp1, Rasgrp1, Cml2, Cml2, Galnt7, Galnt7, Tmem90a, Tmem90a, Abca1, Abca1, Igf2r, Igf2r, Myo5a, Myo5a, Cln8, Cln8, Galnt14, Galnt14, Serinc5, Serinc5, Spg3a, Spg3a, B4galt1, B4galt1, Chpt1, Chpt1, Sgms1, Sg
FDR 10%	UP	immune respo	15	7.51775148	0.00913106	Cfb, P2ry14, Tap2, Cxcl3, H2-Q6, C3, Cxcl11, Il1rn, Il1rap, Mpa2l, Il6, 5830443L24Rik, Igh, Cxcl5, H2-Q7
FDR 10%	UP	ion transport	22	12.6532544	0.00896141	Slc9a9, Cybb, Scn9a, Kcnk10, Ttyh1, Trpm1, Slc40a1, Slc39a11, Kcna2, Atox1, Slc39a6, Cp, Kcnj5, Slc5a3, Tmem38a, Slc41a2, Hcn1, Slc31a1, Cftr, Kcne4, Slc4a4, Scnn1g
FDR 10%	UP	lipid	22	10.0757396	0.00056656	Mtmr10, Acadsb, Acot12, Acsl4, Lipa, Acsf2, Acad11, Asah2, Ugcg, Abca1, Il1rn, Cln8, Osbpl6, Serinc5, Pla2g7, Chpt1, Sgms1, Ehhadh, Atp8a1, Soat1, Enpp2, Apob
FDR 10%	UP	mitochondrion	21	18.4136095	0.29869622	Acadsb, Cybb, Acsl4, Aass, Slc25a20, Endog, Ak3l1, Acsf2, Vps25, Rnasel, Asah2, Nudt9, Ivd, Slc5a3, Araf, Dbi, Ehhadh, Car5b, Oat, Ctsb, Dnm3
FDR 10%	UP	oxidation	10	5.83846154	0.0699215	Fmo1, Ugdh, Acadsb, Cybb, Enox1, Xdh, Acad11, Ivd, Ehhadh, Ero1l
FDR 10%	UP	protein transp	10	10.9934911	0.66373355	Sytl3, Rph3a, Tap2, Vps25, Apobec1, Rab3c, Scamp5, Mcfd2, Apob, Nup93
FDR 10%	UP	proteolysis	18	10.4662722	0.01883408	Cradd, Ctss, Tgm2, Cfb, Cpxm2, St14, Pappa, Lonrf3, Cpd, Gpr26, Gm13, Casp3, Igh, Eps8, Plau, Lgmn, Eps8, Ctsb
FDR 10%	UP	signal transdu	47	28.6260355	0.00057239	Cradd, Wnt5b, Adora2b, Chn1, Ptger4, Psd4, Clec1b, Elmo1, Cblc, Gnal, P2ry14, Rasal2, Fzd3, Fga, Gm266, Cish, Rasgrp1, Sdcbp, Ngfr, Rgs1, Fzd4, Ppp2r2b, Rhpn2, Ms4a4c, Socs2, Pde7b, Hif1a, Gem, Rerg, Il1rn, Fgl2, Il1rap, Gpr26, Rab3c, Tnfrsf11b, Atf6, Its
FDR 10%	UP	signaling	44	32.0627219	0.02040958	Dapp1, Tgm2, Car8, Wnt5b, Entpd2, Pdzd8, Adora2b, Chn1, Ptger4, Dkk3, Csf2rb, AW551984, Lmbr1, Gnal, P2ry14, Tbc1d4, Fzd3, Gpr116, Cish, Rasgrp1, Ngfr, Rgs1, Pik3c3, Fzd4, Rhpn2, Socs2, Hif1a, Itga6, Gfra3, Il1rap, Gpr26, Penk1, Itsn1, Gpr135, Adm2, Araf,
FDR 10%	UP	small GTPase	8	5.03786982	0.13405571	Rasal2, Gm266, Rasgrp1, Gem, Rerg, Rab3c, Itsn1, Rap2b
FDR 10%	UP	synapse	7	4.43254438	0.1574244	Rph3a, Itsn1, Dlg2, Scamp5, Synpr, Gad2, Syt10
FDR 10%	UP	transcription	33	45.3408284	0.98258265	Hopx, Xbp1, Prrx1, Ncoa7, Hltf, Runx1, Ankrd56, Grhl1, Fli1, Ttyh1, Id4, Hsbp1, Vgll4, Vps25, Hif1a, Ikzf4, Fabp4, Mtf2, Bptf, Phtf2, Atf6, Il6, Jun, Smarcb1, Trim24, Myo3a, Sox11, Pde8b, Spic, Rps6ka5, Zfp697, Trappc2, Tle4
FDR 10%	UP	vesicle	12	6.50236686	0.0314058	Wipi1, Hrb, Slc40a1, Rph3a, Igf2r, Rab3c, Scamp5, Synpr, Gad2, Wipf1, Syt10, Atp8a1
FDR 10%	DOWN	adhesion	10	5.77378243	0.06559745	Mybph, Cntnap2, Reln, Cd24a, L1cam, Cadm1, Jup, Cxadr, Cntn1, Hnt
FDR 10%	DOWN	cell cycle	9	6.40987711	0.19407487	Ccna2, Dab2ip, S100a6, Cks2, Cadm1, Setd8, Lin9, Cdca8, Chfr
FDR 10%	DOWN	cell differentia	14	7.4569868	0.01820017	Reln, Cd24a, Stmn1, Anpep, L1cam, Bcl11a, Utp14b, Il11ra1, Cadm1, Rorc, Dapl1, Pappa2, Hhex, Clu
FDR 10%	DOWN	cell division	5	2.40737369	0.09467112	Ccna2, Cks2, Setd8, Cdca8, Chfr
FDR 10%	DOWN	cytoskeleton	13	4.83431953	0.00122056	Lyst, Myo15b, Plek2, Ptpn13, Trib2, Fhod3, Jup, Mlph, Ttll10, Myo5b, Cotl1, Epb4.1l2, Kalrn
FDR 10%	DOWN	development	23	16.606964	0.07004957	Etv1, Ctf1, Reln, Cd24a, Dok7, Stmn1, Anpep, Th, Six4, L1cam, Shisa2, Utp14b, Il11ra1, Cadm1, Plxna1, Rorc, Pcsk9, Car10, Cxadr, Nes, Cr1l, Hhex, Clu
FDR 10%	DOWN	endoplasmic re	9	7.7016386	0.36487206	Adora1, Emid1, Shisa2, Utp14b, Pcsk9, Degs2, Itpr3, Sulf2, Rcn1
FDR 10%	DOWN	immune respo	7	3.76763769	0.08507136	Cd24a, Ccl27, Cadm1, Il1r1, Cr1l, Ccl27, Cxcl16
FDR 10%	DOWN	ion transport	11	6.3413746	0.05468407	Adora1, Slc30a8, Kcnk16, Kcnh1, Slco1a6, Slc4a7, Kcnj6, Fxyd3, Itpr3, Slc22a23, Gria2
FDR 10%	DOWN	lipid	6	5.04961311	0.39286149	Adora1, Utp14b, Acot2, Pcsk9, Degs2, Acaa2
FDR 10%	DOWN	mitochondrion	9	9.22826582	0.57824753	Atpif1, Glul, Utp14b, Acot2, Gpd2, Ptrh2, Acaa2, Aldh2, Tat
FDR 10%	DOWN	protein transp	6	5.50955849	0.47426247	Lyst, Selenbp1, Rab37, Mlph, Rab27b, Xpo7
FDR 10%	DOWN	proteolysis	6	5.24533455	0.4277178	Fap, Anpep, Mela, Pcsk9, Pappa2, 4931433A01Rik
FDR 10%	DOWN	signal transdu	22	14.3463814	0.03035281	Adora1, Lyst, Cntnap2, Reln, Gpr19, Cd24a, Arhgef2, Kcnh1, Dab2ip, Gab1, L1cam, Vipr1, Braf, Npas3, Plxna1, Rab37, Eps8l2, Il1r1, Rab27b, Rgs11, Kalrn, Ghsr
FDR 10%	DOWN	signaling	21	16.0687301	0.12586368	Adora1, Ptprg, Gpr19, Cd24a, Stmn1, Plek2, Arhgef2, L1cam, Vipr1, Braf, Insrr, Med13, Ptprt, Il11ra1, Spsb4, Il1r1, Adcy7, Rgs11, Cntn1, Hhex, Ghsr
FDR 10%	DOWN	transcription	24	22.723259	0.4203575	Fev, Irx2 Etv1, Tox, Tardbp, Chd5, Ccna2, Tanc2, Mlxipl, Six4, Kcnh1, Bcl11a, Braf, Med13, Npas3, Hdac6, Rorc, Rab37, Setd8, Ercc8, Tpbg, Ing2, Tox3, Hhex
FDR 10%	DOWN	ubiquitin	6	5.2257624	0.42424131	Stub1, Usp29, Ube2v2, Hdac6, Spsb4, Chfr
FDR 5%	UP	adhesion	12	5.88120164	0.0156653	Cldn1, B4galt1, Cpxm2, Pcdha1, Amigo2, Icam1, Cldn2, Cdh17, Igfals, Cntn3, Itga6, Cldn8
FDR 5%	UP	apoptosis	9	7.08734638	0.27972167	Cradd, Tnfrsf11b, B4galt1, Il6, Acvr1c, Chpt1, Elmo1, Tnfaip8, Ngfr
FDR 5%	UP	cell cycle	4	6.52913063	0.89490189	Tpd52l1, Araf, Smarcb1, Id4
FDR 5%	UP	cell differentia	8	7.59572144	0.49128026	Hopx, Il6, Acvr1c, Smarcb1, Xdh, Rasgrp1, Ngfr, Efna5
FDR 5%	UP	cell junction	9	3.30942194	0.00628947	Cldn1, Dlg2, Panx1, Gad2, Synpr, Syt10, Rph3a, Cldn2, Cldn8
FDR 5%	UP	cytoskeleton	9	4.92426036	0.06013805	Palld, Pstpip2, Sntg2, Elmo1, Myo3a, Epb4.1l4a, Rph3a, Cttnbp2, Svil
FDR 5%	UP	development	16	16.9159308	0.62887424	Hopx, G6pd2, Runx1, B4galt1, Acvr1c, Scn9a, Smarcb1, Grhl1, Sftpd, Id4, Ngfr, Crybb3, Ppp2r2b, Apob, Gfra3, Efna5
FDR 5%	UP	endoplasmic re	15	7.8449249	0.0127237	Fmo1, Edem3, Ugt1a1, Serinc5, Atf6, Minpp1, Rasgrp1, Soat1, Mcfd2, Apob, Trappc2, B3galt5, Ero1l, Cldn8
FDR 5%	UP	fatty acid	1	1.50518889	0.78084041	Ehhadh
FDR 5%	UP	Golgi	26	13.1978152	0.00074747	Serinc5, Serinc5, B4galt1, B4galt1, Chst9, Chst9, Chpt1, Chpt1, B3galnt1, B3galnt1, Wipi1, Wipi1, Gad2, Gad2, St3gal5, St3gal5, Rasgrp1, Rasgrp1, B3galt1, B3galt1, Mcfd2, Mcfd2, Trappc2, Trappc2, B3galt5, B3galt5
FDR 5%	UP	immune respo	10	3.83773327	0.00545872	Cxcl11, Il1rap, Mpa2l, Il6, Mpa2l, P2ry14, 5830443L24Rik, Igh, Cxcl5, C3
FDR 5%	UP	ion transport	14	6.45935366	0.00568632	Slc9a9, Slc39a11, Kcna2, Cp, Kcnj5, Tmem38a, Scn9a, Slc41a2, Hcn1, Slc31a1, Cftr, Trpm1, Kcne4, Scnn1g
FDR 5%	UP	lipid	9	5.1435594	0.07445451	Mtmr10, Osbpl6, Serinc5, Chpt1, Ehhadh, Atp8a1, Soat1, Enpp2, Apob
FDR 5%	UP	mitochondrion	7	9.39995448	0.83447788	Ivd, Araf, Ak3l1, Ehhadh, Car5b, Oat, Ctsb
FDR 5%	UP	oxidation	6	2.98047337	0.07957658	Fmo1, Ivd, Enox1, Ehhadh, Xdh, Ero1l
FDR 5%	UP	protein transp	6	5.6120619	0.49203526	Sytl3, Rph3a, Mcfd2, Apob, Nup93, Apobec1
FDR 5%	UP	proteolysis	7	5.34292217	0.28767464	Cradd, Lonrf3, Gpr26, Cpxm2, Igh, Lgmn, Ctsb
FDR 5%	UP	signal transdu	28	14.6132909	0.00071478	Cradd, Rerg, Fgl2, Il1rap, Gpr26, Adora2b, Ptger4, Tnfrsf11b, Atf6, Clec1b, Gpr135, Elmo1, Araf, Cblc, Il13ra1, Rap2b, Gpr126, P2ry14, Rasal2, Ms4a6b, Cish, Cxcl5, Pde8b, Rasgrp1, Ngfr, Ppp2r2b, Socs2, Pde7b
FDR 5%	UP	signaling	26	16.3676832	0.01292881	Dapp1, Car8, Il1rap, Entpd2, Gpr26, Pdzd8, Adora2b, Ptger4, Penk1, Gpr135, Adm2, Araf, Gpr126, P2ry14, Mtap7d2, Ahnak, Tbc1d4, Csf2rb, Cish, Rasgrp1, Ngfr, Prkd1, Socs2, Itga6, Tle4, Gfra3
FDR 5%	UP	small GTPase	4	2.5717797	0.25683702	Rerg, Rap2b, Rasal2, Rasgrp1
FDR 5%	UP	synapse	5	2.26276741	0.07744062	Dlg2, Gad2, Synpr, Syt10, Rph3a
FDR 5%	UP	transcription	18	23.1460173	0.89734076	Hopx, Ncoa7, Phtf2, Hltf, Runx1, Atf6, Il6, Smarcb1, Grhl1, Myo3a, Sox11, Id4, Pde8b, Spic, Rps6ka5, Zfp697, Trappc2, Tle4
FDR 5%	UP	vesicle	6	3.31939008	0.11687146	Wipi1, Gad2, Synpr, Syt10, Atp8a1, Rph3a
FDR 5%	DOWN	adhesion	4	1.63814292	0.08122878	Cadm1, Cntn1, Jup, Reln
FDR 5%	DOWN	cell cycle	1	1.8186163	0.84258056	Cadm1
FDR 5%	DOWN	cell differentia	8	2.11570323	0.00117104	Il11ra1, Cadm1, Pappa2, Rorc, Dapl1, Reln, Utp14b, Anpep
FDR 5%	DOWN	cytoskeleton	3	1.37159763	0.15773544	Ptpn13, Jup, Mlph
FDR 5%	DOWN	development	10	4.71174329	0.01773934	Il11ra1, Cadm1, Rorc, Etv1, Six4, Pcsk9, Reln, Dok7, Utp14b, Anpep
FDR 5%	DOWN	endoplasmic re	6	2.18511607	0.02167707	Adora1, Rcn1, Pcsk9, Emid1, Utp14b, Itpr3
FDR 5%	DOWN	immune respo	3	1.06895767	0.09152767	Cadm1, Ccl27, Ccl27
FDR 5%	DOWN	ion transport	7	1.7991807	0.002062	Adora1, Kcnh1, Gria2, Fxyd3, Slc30a8, Kcnj6, Itpr3
FDR 5%	DOWN	lipid	3	1.43268093	0.17257546	Adora1, Pcsk9, Utp14b
FDR 5%	DOWN	mitochondrion	2	2.61825216	0.74329438	Tat, Utp14b
FDR 5%	DOWN	protein transp	3	1.56317706	0.20552603	Selenbp1, Mlph, Xpo7
FDR 5%	DOWN	proteolysis	3	1.4882112	0.18640546	Pappa2, Pcsk9, Anpep
FDR 5%	DOWN	signal transdu	7	4.07036869	0.11056519	Adora1, Npas3, Kcnh1, Eps8l2, Reln, Gpr19, Ghsr
FDR 5%	DOWN	signaling	5	4.55903505	0.48327762	Adora1, Il11ra1, Cntn1, Gpr19, Ghsr
FDR 5%	DOWN	transcription	8	6.44706418	0.31459057	Npas3, Mlxipl, Rorc, Etv1, Six4, Kcnh1, Tox, Tpbg

Supplementary Methods

X-gal staining and immunohistochemistry in pancreas and islets

Embryo (E15.5) and adult (8 weeks of age) pancreata and ECM-plated islets were washed with PBS and fixed immediately in 4% paraformaldehyde at 4°C overnight or 10 min for ECM plated islets. For X-GAL staining, we fixed 10 min after dissection, and then we submerged the tissue for 4 h in X-gal solution (40 mg X-GAL/ml DMSO, diluted 1:40 in 5 mM $K_3Fe(CN)_6$, 5 mM $K_4Fe(CN)_6$, 2 mM $MgCl_2$ in PBS). Finally, we fixed the tissue overnight in 4% paraformaldehyde. For immunostaining, we embedded the tissue in paraffin and cut sections 5 µm thick. Then, sections were hydrated and boiled for 15 min in 0.01 mol/l sodium citrate pH 6, and the endogenous peroxidase activity was inhibited with 3% H_2O_2 for 30 min, only for colorimetric detection. Next, sections were permeabilized with TBS 0.05% Tween 20. Blocking was performed with milk or 10% normal goat serum for 1 h; finally, the primary and secondary antibodies were incubated overnight and 1 h, respectively. In the colorimetric method, sections were incubated with biotinylated secondary antibody, and detection was performed with the Vectastain ABC kit (Vector Laboratories, Burlingame, CA), followed by incubation with diaminobenzidine (DAB) peroxidase substrate (Sigma).

Morphometric quantification of islets and cell numbers

E15.5 pancreata from 3 Pdx1Cre;*Pparb/d*$^{fl/fl}$ and 3 *Pparb/d*$^{fl/fl}$ embryos were cut in 2–4 sections of 5 µm thickness every 75 µm. The Neurog3- or insulin-positive cells were counted from all the sections by using a standard fluorescence microscope at 10X (Neurog3) or 20X (insulin) magnification. The cell number was normalized by epithelial e-cadherin expressing area, and determined using ImageJ software. Pancreata from 3 Pdx1Cre;*Pparb/d*$^{fl/fl}$ and 3 *Pparb/d*$^{fl/fl}$ 8-week-old mice were processed to determine the islet β-cell mass. 18 (6 per mouse) insulin-stained (colorimetric method) sections of 5 µm thickness separated by 150 µm

were scanned by a digital Coolscope microscope (Nikon Corporation) at 10X magnification. Then, we calculated the area of islets (more than 5 cells) from whole sections, using ImageJ software. The total islet area was divided by the total pancreas area to obtain the relative insulin cell surface, which was multiplied by the weight of the pancreas to get the β-cell mass. To determine the α-cell mass we processed glucagon-stained sections as above.

Capacitance measurements

Measurements of exocytosis were performed in the whole-cell configuration using an EPC-9 amplifier controlled by Pulse software (both HEKA Elektronik, Germany). The intracellular solution consisted of (in mM) 125 CsCl, 10 NaCl, 1 MgCl2, 3 ATP-Mg, 0.1 cAMP, 0.05 EGTA, and 5 HEPES (pH 7.15). The extracellular solution was (in mM) 138 NaCl, 5.6 KCl, 1.2 MgCl2, 2.6 CaCl2, 3 D-glucose, and 10 mM HEPES (pH 7.40) and held at 32°C. Capacitance was measured using 500 Hz, 20-mV sine waves around -70 mV and calculated offline. β-Cells were identified through their electrophysiological properties (2).

Intracellular Ca^{2+} imaging

Islets were dispersed using Ca^{++} free buffer, then cultured for 48 h. Dispersed islets were incubated for 30 min in KRBH containing 3 mM glucose and 200 nM FURA-RED AM (Invitrogen, UK). Cells were stimulated using the conditions indicated and excited at 480/440 nm using an Olympus IX-81 microscope coupled to an F-view camera and captured using Cell R software (Olympus, UK) and a 40X oil immersion objective. Data are expressed as the ratio of the fluorescence emission at 440/480 nm. The area under the curve (AUC) and height of the response were calculated using OriginPro7.5 software (OriginLab, Northampton, MA), and statistical analysis was performed with t-tests using GraphPad Prism 4.0 (GraphPad Software Inc.).

Microarray and TaqMan qRT-PCR

Total RNA from islets or pancreas was extracted by using guanidine thiocyanate (Sigma) according to the manufacturer's recommendation. RNA quality and quantity was assessed by NanoDrop®ND-1000 spectrophotometer and an Agilent 2100 bio-analyzer. For the analysis of gene expression by TaqMan, we generated the cDNA from 200 ng of total RNA by using Super-Script III RT (Invitrogen, UK). PCR amplification was performed by using mouse-specific TaqMan probes (Applied Biosystems) on an Applied Biosystems 7900 HT SDS qRT-PCR system. Three biological samples were run in triplicate to assess the technical variability. For each sample of microarray analysis, 5 ng of total islet RNA was amplified and labeled using the GeneChip IVT labeling kit according to the protocol provided by the supplier. Affymetrix (Santa Clara, CA, USA) Mouse Genome 430 2.0 arrays were hybridized with 10 μg of labeled cRNA, washed, stained, and scanned according to the protocol described in the Affymetrix GeneChip® Expression Analysis Manual (Fluidics protocol EukGeWS2v5_450). All the statistical analyses were performed using the free high-level interpreted statistical language R (http://www.R-project.org) and various Bioconductor packages (http://www.Bioconductor.org). Normalized expression signals were calculated from Affymetrix CEL files using the RMA normalization method implemented in the "affy" package (3,4). Differential hybridized features were identified using the Bioconductor package "limma" that implements linear models for microarray data (5). *P* values were then adjusted for multiple testing with Benjamini and Hochberg's method to control FDR.

The procedure to test for enrichment of GO annotation terms was performed separately on up- and downregulated genes as follows. First, the number of occurrences of the different Biological Process and Cellular Component GO categories was counted in the lists of regulated genes at FDR 5% and FDR 10% after removing duplicated genes. Single words like

"lipid" or composite terms like "immune response" were selected among the GO terms found in the top 5% of the occurrence lists. The goal of this procedure was to extract informative terms that would represent general aspects of the cellular physiology and give insight into the functions affected by the KO. We selected a list of 24 terms or words for the upregulated genes and a list of 17 terms or words for the downregulated genes. These selected terms were tested for enrichment in regulated genes using a Fisher's exact test. To construct contingency tables, duplicated genes were removed. Then, we counted the number of genes on the array having a particular term in its GO annotations, as well as the number of regulated genes having a particular term in its GO annotations. Because only a few terms were tested, p values were not adjusted for multiple testing. Table S2 contains all the words tested for enrichment in the GO annotation. GO annotations contained on the Affymetrix annotation na26 were used.

Supplemental Tables

Supplemental Table 2. GO enrichment term

Supplemental References

1. Cramer LP, Briggs LJ, Dawe HR. Use of fluorescently labelled deoxyribonuclease I to spatially measure G-actin levels in migrating and non-migrating cells. *Cell Motil Cytoskeleton.* 2002;51(1):27-38.
2. Barg S, Galvanovskis, J., Göpel, SO., Rorsman, P., Eliasson, L. Tight coupling between electrical activity and exocytosis in mouse glucagon-secreting alpha-cells. *Diabetes.* 2000;49(9):1500-1510.

3. Bolstad B, Irizarry, RA., Astrand, M., Speed, TP. A comparison of normalization methods for high density oligonucleotide array data based on variance and bias. *Bioinformatics.* 2003;19(2):185-193.

4. Irizarry R, Hobbs, B., Collin, F., Beazer-Barclay, YD., Antonellis, KJ., Scherf, U., Speed, TP. Exploration, normalization, and summaries of high density oligonucleotide array probe level data. *Biostatistics.* 2003;4(2):249-264.

5. Smyth G. Linear models and empirical bayes methods for assessing differential expression in microarray experiments. *Stat Appl Genet Mol Biol.* 2004;3:Article3.